Role of Calcium in Maintaining the Heme Environment of Manganese Peroxidase[†]

Greg R. J. Sutherland,[‡] Laura Schick Zapanta,[§] Ming Tien,[§] and Steven D. Aust*,[‡]

Biotechnology Center, Utah State University, Logan, Utah 84322-4705, and Department of Biochemistry and Molecular Biology and Center for Biomolecular Structure and Function, Pennsylvania State University, University Park, Pennsylvania 16802

Received August 28, 1996; Revised Manuscript Received November 27, 1996[⊗]

ABSTRACT: We previously demonstrated that manganese peroxidase from the white-rot fungus *Phanerochaete chrysosporium* was very susceptible to thermal inactivation due to the loss of calcium from the enzyme [Sutherland & Aust (1996) *Arch. Biochem. Biophys. 332*, 128−134]. The structural changes that occur during thermal inactivation and the release of calcium from manganese peroxidase have now been characterized. Thermal inactivation caused distinct alterations in the heme environment and slight changes in the overall protein structure, both of which were reversed upon reactivation of the enzyme with calcium. The absorption spectrum of inactivated manganese peroxidase was similar to that of low-spin ferric heme proteins, indicating that a sixth ligand had bound to the distal side of the heme iron. Consistent with disruption of the distal heme environment, thermally inactivated manganese peroxidase did not react with hydrogen peroxide to form compound I. The inactive enzyme exhibited a pH-dependent absorption transition with a pK_a of 5.7. Studies involving imidazole indicated that the sixth ligand may be a distal histidine. Low-temperature electron paramagnetic resonance spectroscopy confirmed that the heme iron of the inactivated form of manganese peroxidase was predominantly in a low-spin state. The near-ultraviolet/visible circular dichroism spectrum also supported the proposed formation of a highly symmetric bis(imidazole) heme complex upon thermal inactivation of the enzyme. A recombinant manganese peroxidase, in which the distal calcium binding site was altered such that calcium binding would be minimized, was also characterized. This enzyme, D47A, had the same catalytic and spectroscopic properties and calcium content as thermally inactivated manganese peroxidase. Therefore, the inactivation and structural changes that occurred during thermal incubation of manganese peroxidase could be explained by the loss of the distal calcium.

White-rot fungi produce and secrete heme-containing peroxidase enzymes which are believed to be responsible for the degradation of lignin and a wide variety of environmental pollutants by these fungi (Barr & Aust, 1994; Tien, 1987). The two types of peroxidases produced by the white-rot fungus *Phanerochaete chrysosporium* that have been purified and characterized are manganese peroxidase (MnP)[1] and lignin peroxidase (LiP) (Tien, 1987). The MnP isozymes oxidize Mn^{2+} to Mn^{3+}, which can then act as a diffusible oxidant (Glenn et al., 1986; Wariishi et al., 1988). The production of Mn^{3+} by the extracellular degradation system of white-rot fungi has been proposed to be particularly important for the degradation of sterically bulky compounds which are unable to access the active site of the peroxidases (Wariishi et al., 1988).

The catalytic cycle of MnP is similar to that of other peroxidases (Tien, 1987). The first step of the cycle involves the oxidation of the ferric, or resting, form of the enzyme by two electrons by hydrogen peroxide (H_2O_2). This results in the formation of the enzyme intermediate referred to as compound I, which is an oxyferryl porphyrin π cation radical intermediate. The heme iron is coordinated on the proximal side by His173 but is not liganded on the distal side (Sundaramoorthy et al., 1994). This enables oxygen of H_2O_2 to bind to the heme iron during compound I formation (Dunford, 1991). The amino acids His46 and Arg42 of the distal heme environment have also been proposed to be involved in the reaction of ferric MnP with H_2O_2 (Dunford, 1991; Sundaramoorthy et al., 1994). Once formed, compound I can be reduced back to the ferric form, via compound II, as 2 equiv of Mn^{2+} are sequentially oxidized. The oxidation of Mn^{2+} is believed to occur at the heme edge rather than in the H_2O_2 binding site of the distal heme environment (Kishi et al., 1996; Sundaramoorthy et al., 1994).

Analysis of the crystal structure of MnP revealed the presence of two calcium ions (Sundaramoorthy et al., 1994). One calcium was reported to be tightly bound on the proximal side of the heme while the other calcium was bound on the distal side of heme and was considered to be loosely bound. Due to the relatively close proximity of the calcium ions to the heme, they were proposed to be important for the stabilization of the active site of the enzyme.

We recently demonstrated that MnP was particularly susceptible to thermal inactivation due to the loss of calcium from MnP (Sutherland & Aust, 1996). During thermal inactivation calcium was released from MnP, and inactivation

[†] This work was supported by NIEHS Superfund Basic Research and Training Grant ES04922, NSF Grant BIR-9413530, and U.S. Department of Energy Grant DE-FG02-87ER13690.

* To whom correspondence should be addressed.

[‡] Utah State University.

[§] Pennsylvania State University.

[⊗] Abstract published in *Advance ACS Abstracts,* March 15, 1997.

[1] Abbreviations: MnP, manganese peroxidase; LiP, lignin peroxidase; EGTA, ethylene glycol bis(β-aminoethyl ether)-*N*,*N*,*N*′,*N*′-tetraacetic acid; D47A, the Asp47 mutant of recombinant MnP from *E. coli*; ICP, inductively coupled plasma; EPR, electron paramagnetic resonance; CD, circular dichroism; MnP−CN, cyanide adduct of manganese peroxidase; CCP, cytochrome *c* peroxidase; CT, charge-transfer band in electronic absorption spectrum of manganese peroxidase.

S0006-2960(96)02195-2 CCC: $14.00

could be prevented and reversed in the presence of calcium. Thermally inactivated MnP had one remaining calcium, which was predicted to be the tightly bound calcium in the proximal site. Analysis of the crystal structure of MnP revealed that the distal calcium was liganded by Asp47 of helix B, which also contained residues proposed to be involved in the binding of H_2O_2 (His46 and Arg42) and Mn^{2+} (Glu35 and Glu39) to ferric MnP (Sundaramoorthy et al., 1994). Therefore it was predicted that the removal of the distal calcium may disrupt the position of helix B such that MnP would no longer be active (Sutherland & Aust, 1996). In this investigation we have characterized the structural changes that occur during the thermal inactivation and loss of calcium from MnP. To further investigate the role of the distal calcium in maintaining the heme environment, we have characterized a recombinant form of MnP in which Asp47, a ligand of the distal calcium, was changed to an alanine to reduce the affinity of this site for calcium.

MATERIALS AND METHODS

Chemicals. Hydrogen peroxide, calcium chloride, imidazole, ethylene glycol bis(*β*-aminoethyl ether)-*N*,*N*,*N*′,*N*′-tetraacetic acid (EGTA), and Trizma base were purchased from Sigma Chemical Co. (St. Louis, MO). Tris hydrochloride, potassium cyanide, and dibasic and monobasic sodium phosphate were purchased from Mallinckrodt (Paris, KY). DEAE Bio-Gel A was purchased from Bio-Rad (Hercules, CA). All solutions were prepared using purified water (Barnstead NANOpure II system; specific resistance 18.0 MΩ·cm^{-1}). All buffers were passed through a column of Chelex 100 (Bio-Rad, Richmond, CA).

Enzyme. Pure manganese peroxidase isozyme H4 was produced from liquid cultures of *P. chrysosporium* as previously described (Tuisel et al., 1990). The enzyme concentration was determined using the extinction coefficient at 406 nm of 127 mM^{-1} cm^{-1} (Millis et al., 1989).

The activity of MnP was assayed by monitoring the production of manganese^{3+}−oxalate using conditions previously described (Sutherland et al., 1996). Unless stated otherwise, the thermal incubations of the enzymes were carried out by placing enzyme mixtures, contained in plastic vials, in a circulating water bath. Absorption spectra were acquired in a Shimadzu UV-2101PC scanning spectrophotometer at room temperature. The scan speed was 6 nm/s unless otherwise stated.

Production and Purification of D47A. Site-directed mutagenesis was used to replace aspartic acid residue 47 of recombinant MnP with alanine using the recombinant MnP expression vector constructed by Whitwam et al. (1995). The protein was expressed and refolded in *E. coli* as previously reported (Whitwam & Tien, 1996). The refolding mixture was dialyzed extensively against 50 mM Tris and 10 mM $CaCl_2$, pH 8. The recombinant protein was purified by anion-exchange chromatography on DEAE Bio-Gel A (1.5 × 20 cm) using a linear gradient of 10−150 mM $CaCl_2$ in 50 mM Tris, pH 8. Column fractions with a high rate of absorbance at 407 nm to absorbance at 280 nm (R_z) were pooled and dialyzed against 50 mM Tris, pH 8. The purified D47A had an R_z value of 2.4.

Determination of Calcium Concentration in MnP. The amount of calcium in the MnP samples was determined by inductively coupled plasma (ICP) emission spectroscopy by the Utah State University Analytical Laboratory using a Thermo Jarrell Ash ICAP-9000 (Franklin, MA). The values represent the average and standard deviation of at least three samples, except for the data for the D47A sample, which is reported as the average and standard error of two samples due to the limited amount of the enzyme.

Compound I Formation. The formation of compound I under pseudo-first-order conditions was monitored at 417 nm using a KinTek Instruments three-syringe stopped-flow spectrophotometer (State College, PA). A detailed description of the operation of this instrument has previously been published (Kuan et al., 1993).

Electron Paramagnetic Resonance Spectroscopy. All EPR spectra were acquired using a Bruker ESP300 spectrometer equipped with an Oxford ESR 10 helium flow cryostat and a DTC-2 temperature controller. The enzyme samples were concentrated using Centricon-10 concentrators (Amicon, Inc., Beverly, MA).

Circular Dichroism Spectroscopy. All CD spectra were acquired on an Aviv Model 62DS CD spectrometer at room temperature. The data was collected every 0.5 nm using a spectral band width of 0.7 nm in the far-UV region (190−260 nm). In the near-UV/visible region (250−650 nm) data were collected every 1.0 nm at a band width of 1.0 nm. The molar ellipticity values reported were calculated using protein molarity. Background spectra of buffers and other reagents were subtracted from the spectra of the enzyme samples. The CD spectra recorded in the far-UV region were analyzed for secondary structure using the Variable Selection computer program designed by W. C. Johnson at Oregon State University.

RESULTS

Thermal Inactivation. Absorption spectra acquired during the thermal inactivation of MnP are shown in Figure 1A. The inactivation was carried out in the spectrophotometer cuvette at pH 7.5 and 35 °C over 20 min in the presence of 0.10 mM EGTA. The changes in the absorption spectrum of MnP during thermal inactivation are consistent with changes in the heme environment. A red shift was observed in the Soret absorption maximum from 407 to 412 nm and there was a corresponding decrease in absorbance to 68% that of active enzyme (Table 1). In addition, there was a weak absorption maximum at approximately 359 nm that formed during inactivation. There were also distinct changes in the absorption spectrum of MnP at higher wavelengths. During thermal inactivation, the charge-transfer bands at 504 and 637 nm decreased and there was a concomitant increase in absorbance with maxima at 533 and 561 nm. Isosbestic points were observed at 349, 414, 469, 523, and 593 nm. The observed changes in the absorption spectrum were indicative of a conversion from a high-spin to a low-spin ferric heme complex (Hollenberg et al., 1980; Yonetani et al., 1966).

Because thermal inactivation under similar conditions has been shown previously to be due to the release of calcium from MnP (Table 2; Sutherland & Aust, 1996), the effect of calcium on the absorption spectrum of inactive MnP was investigated. The effects of thermal incubation on the absorption spectrum and activity of MnP were reversed upon the addition of calcium (Figure 1B). Calcium was added to

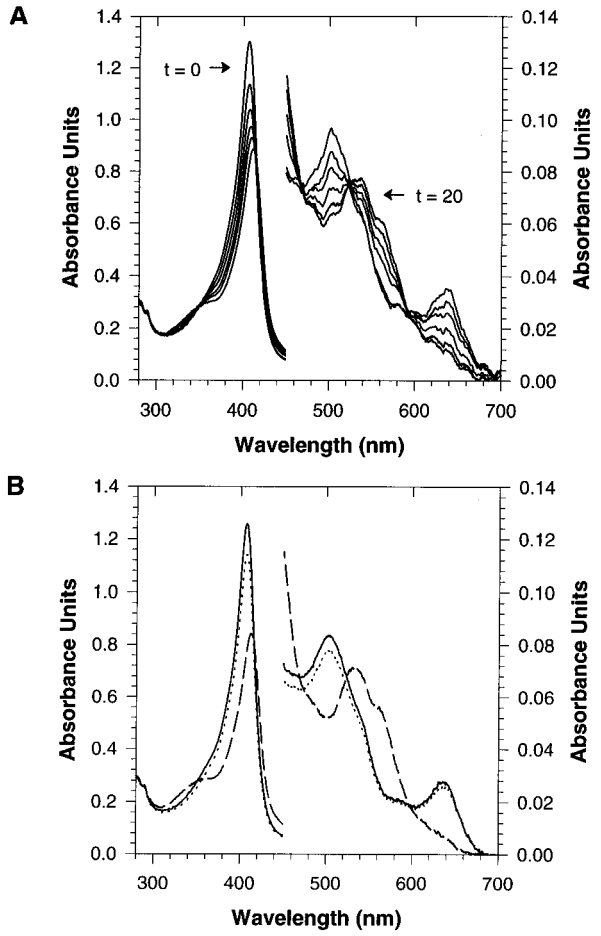

FIGURE 1: Absorption spectra of thermally inactivated and reactivated MnP. (A) Absorption spectra during the thermal inactivation of MnP in the spectrophotometer cuvette at 35 °C in 20 mM Tris, pH 7.5, and 0.10 mM EGTA. The concentration of MnP was 10.2 μM. The traces were acquired at 0, 0.5, 1.0, 4.0, 9.0, and 20 min, at a scan speed of 18 nm/s, and the corresponding enzyme activities were 100%, 72%, 46%, 28%, 16%, and 3%. (B) Absorption spectra of 9.9 μM MnP, active (—), thermally inactivated (---), and calcium reactivated (•••). The MnP was thermally inactivated at 37 °C in 20 mM Tris, pH 7.5, and 1.0 mM EGTA for 3.5 min to 2% activity. The inactivated MnP was reactivated to 91% activity following the addition of 1.5 mM $CaCl_2$ and incubation at 30 °C for 15 min.

MnP that had been rapidly thermally inactivated in the presence of 1.0 mM EGTA to 2% activity (absorption maxima at 359, 412, 533, and 561 nm), and the activity was recovered to 91%. The absorption spectrum of the reactivated enzyme had maxima at 407, 504, and 637 nm. The absorption at 407 nm of the reactivated MnP was 92% that of the original, fully active enzyme mixture.

Compound I Formation. The reaction of H_2O_2 with thermally inactivated MnP was investigated using single-turnover conditions and compared to that with active MnP. As shown in Figure 2, there was a rapid decrease in absorbance at 417 nm due to the formation of compound I upon mixing 25 equiv of H_2O_2 with the ferric form of active MnP. The k_{obs} for the reaction was 42 s^{-1}, consistent with previously reported data. However, there was no significant decrease in the absorbance at 417 nm upon mixing 25 equiv of H_2O_2 with thermally inactivated MnP over either the time scale of this experiment or longer time.

Cyanide Derivatives of MnP. The absorption spectrum of the cyanide adduct of active MnP (MnP−CN) had a red-shifted Soret maximum (422 nm) in addition to maxima at 359 and 544 nm (Figure 3A, Table 1). The absorption spectrum of inactive MnP also changed significantly upon addition of cyanide (Figure 3B, Table 1). The Soret absorption maximum shifted from 412 to 420 nm and the absorption maxima at 533 and 562 nm disappeared with a concomitant appearance of a maximum at 544 nm. The absorption spectra of the cyanide adducts of inactive and active MnP were comparable but not identical. The addition of excess imidazole to the cyanide adduct of inactive MnP resulted in an enzyme with an absorption spectrum similar to that of inactive MnP in the absence of cyanide or imidazole (Figure 3C, Table 1).

pH Dependence of the Absorption Spectrum of Inactivated MnP. Shown in Figure 4 is the effect of pH on the absorption spectrum of thermally inactivated MnP. While the absorption spectrum of active MnP was not affected by pH in the range 4.0−7.5 (data not shown), the absorption spectrum of inactive MnP was dependent on pH. As the pH decreased, the absorbance of the Soret maximum at 412 nm decreased and blue-shifted, and the absorbance at 359 nm increased. An isosbestic point was observed at 397 nm. The pH-dependent transition exhibited a pK_a of 5.7 (Figure 4, inset). The effect of pH on the absorption spectrum of inactive MnP was reversed by the addition of imidazole. The addition of imidazole to inactive MnP at pH 7.5 had no effect (data not shown), while at pH 4.5, the absorption spectrum shifted and was almost identical to that of inactive MnP at pH 7.5 (Figure 4).

Characterization of D47A. The specific activity of recombinant D47A produced and purified from *E. coli*, was less than 1% compared to active MnP from *P. chrysosporium* and active recombinant wild-type MnP produced from *E. coli*. Compound I formation was also not observed upon the addition of H_2O_2. The absorption spectrum at D47A is shown in Figure 5. The absorption maxima at 359, 412, 533, and 561 nm corresponded to those of thermally inactivated MnP. The addition of calcium to D47A did not result in increased activity or a change in the absorption spectrum. In addition to having the same spectroscopic and catalytic properties as inactive MnP, D47A also contained only one calcium (Table 2).

EPR Spectroscopy. Shown in Figure 6 are the low-temperature EPR spectra of active and thermally inactivated MnP. The EPR spectrum of active MnP had characteristic signals with *g*-values of 6.01 and 1.99 due to high-spin ferric iron in a symmetric environment (Dunford & Stillman, 1976). However, the EPR spectrum of inactive MnP had high-spin ferric signals of much less intensity (∼16%) and signals at $g = 2.94$, 2.29, 2.07, and 1.48 due to low-spin ferric iron, which are typically weaker and broadened (Dunford & Stillman, 1976).

In Figure 7, the EPR spectrum of inactive MnP is shown in comparison to the spectra of inactive MnP at pH 4.5, D47A, and MnP−CN. The spectrum of inactive MnP at pH 4.5 had low-spin signals at $g = 2.89$, 2.49, 2.29, 2.09, and 1.80. The spectrum of D47A was very similar to that of inactive MnP, with a small high-spin ferric signal and low-spin signals with *g*-values of 2.94, 2.30, 2.07, and 1.48. There were no high-spin ferric signals detected in the EPR spectrum of MnP−CN, but the low-spin ferric signals were at $g = 3.23$, 2.21, and 1.77. There was also a small signal at $g \sim 4.3$ in all of the samples with low-spin MnP which

Table 1: Spectroscopic Parameters of MnP[a]

protein[b]	δ[c]	Soret	CT2[d]	β	α	CT1
MnP		407 (127)	504 (8.5)			637 (2.8)
MnP−CN	359 (26)	422 (81)		544 (9.5)		
inactive MnP	359 (29)	412 (86)		533 (7.4)	561 (5.7)	
(inactive MnP)-CN	359 (28)	420 (81)		543 (9.1)		
(inactive MnP)-CN + imidazole[e]	359 (26)	414 (85)		533 (8.0)	565 (6.0)	
D47A	359	412		533	561	

[a] λ_{max} values are in nanometers; extinction coefficients (mM^{-1} cm^{-1}) are given in parentheses. [b] All absorption spectra were recorded at pH 8.0. [c] δ, Soret, CT2, β, α, and CT1 represent the type of the absorption band. [d] CT refers to a charge-transfer band. [e] This sample was (inactive MnP)-CN incubated with imidazole as described in the legend to Figure 3.

Table 2: Amount of Calcium in MnP

enzyme sample	mol of Ca^{2+}/mol of MnP[a]
MnP	3.9 ± 0.2[b]
inactive MnP	1.0 ± 0.1[b]
D47A	1.0 ± 0.1

[a] Concentration of calcium determined by ICP emission spectroscopy. [b] These values were reported previously by Sutherland and Aust (1996). To prepare inactive MnP, the enzyme was inactivated to less than 5% activity at pH 7.1, 37 °C, in the presence of EGTA and then separated from the low molecular weight fraction.

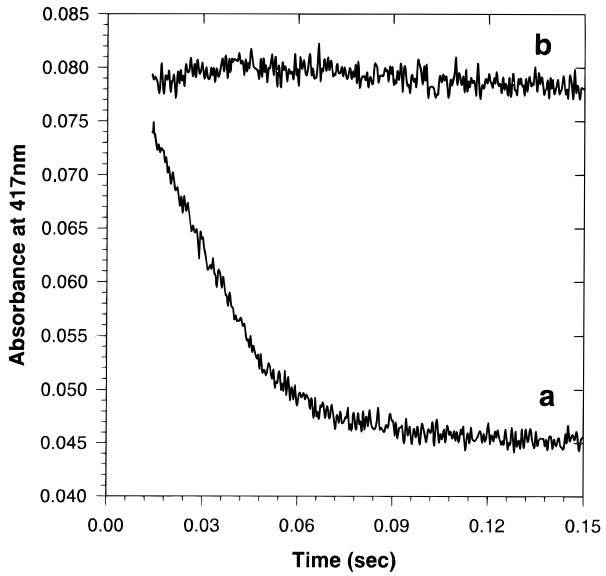

FIGURE 2: Absorbance at 417 nm of active and thermally inactivated MnP upon addition of H_2O_2. (a) Active and (b) thermally inactivated MnP, prepared as described in the legend to Figure 1B, were mixed with 25 equiv of H_2O_2 at pH 7.0 such that the final concentrations in the reaction mixture were 1.0 μM MnP, 25 μM H_2O_2, and 50 mM Tris, pH 7.0.

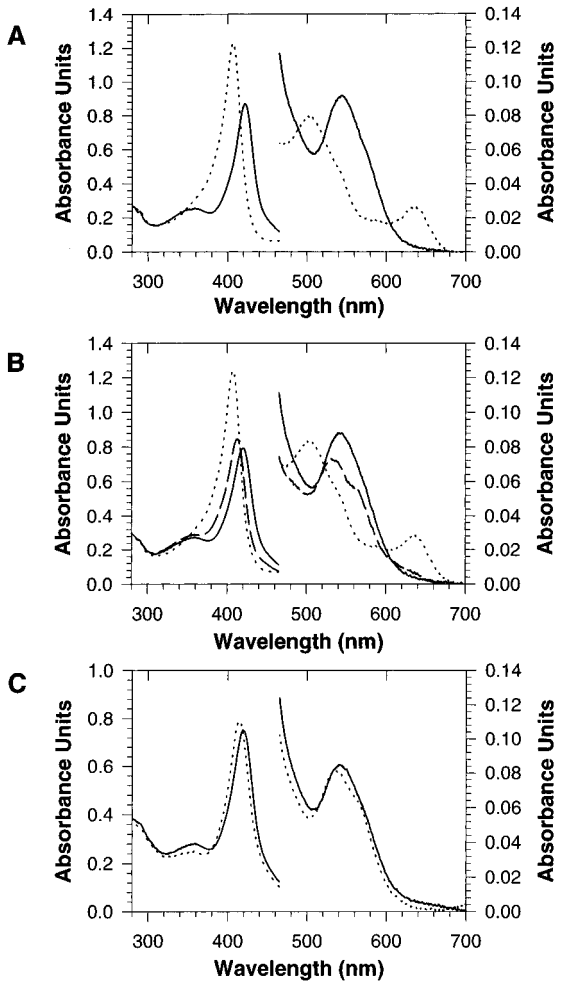

FIGURE 3: Effect of cyanide on the absorption spectrum of active and thermally inactivated MnP. (A) Absorption spectra of active MnP, 9.7 μM, in 20 mM Tris, pH 8.0, in the absence (···) and presence (—) of 5 mM potassium cyanide. (B) Absorption spectra of active MnP, 9.8 μM in 20 mM Tris, pH 8.0 (···). The enzyme sample was inactivated as described in the legend of Figure 1B to 4% activity (---) and then incubated with 5 mM potassium cyanide (—). (C) Absorption spectra of the cyanide adduct of inactive MnP, prepared as in (B), in absence (—) and presence (---) of 50 mM imidazole.

has been observed in other low-spin iron heme proteins and has been attributed to non-heme rhombic iron (Blumberg et al., 1968).

Circular Dichroism. Circular dichroism was utilized to investigate the effects of thermal inactivation on the secondary structure of MnP. As shown in Figure 8A, the far-UV CD spectrum of active MnP had features characteristic of a protein with a large amount of α-helical structure. Computational analysis of the spectrum indicated that active MnP had 35% α-helical content and essentially no β-sheet structure. This was consistent with the crystallographic analysis of MnP which reported that 35% of the amino acids were present in α-helices (Sundaramoorthy et al., 1994). The CD spectrum of thermally inactivated MnP (Figure 8B) differed from that of active MnP. The ellipticity was slightly less at 222 nm but was greater at 208 nm. The results of computational analysis of this spectrum indicated that there was slightly less α-helical structure (26%) in inactive MnP; however, the fit to the data was poor. The alterations in the protein structure of inactive MnP detected by CD were reversed upon reactivation of the enzyme with calcium (Figure 8C).

The heme environment of the active and inactive forms of MnP were further compared by analyzing the CD spectra in the near-UV/visible region. The CD spectrum of active MnP from 250 to 650 nm (Figure 9A) exhibited negative

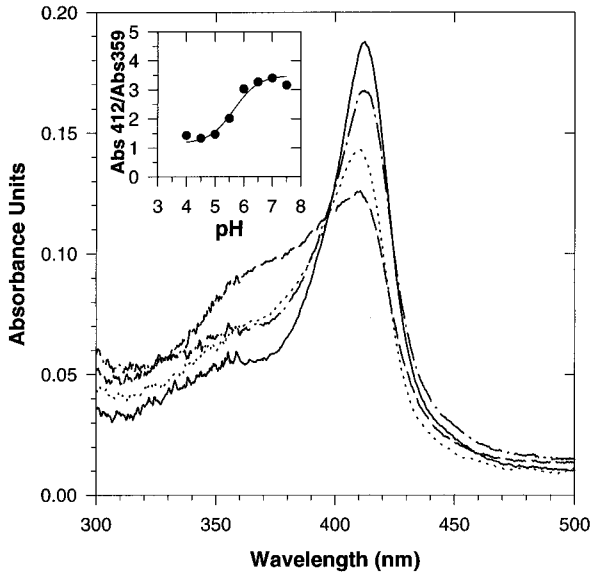

FIGURE 4: Effect of pH on the absorption spectrum of thermally inactivated MnP. Inactivated MnP, prepared as described in the legend of Figure 1B, was diluted in excess sodium phosphate buffer of varying pH such that the final concentrations were 2.2 μM MnP and 50 mM phosphate, pH 7.5 (—), pH 5.5 (•••), and pH 4.5 (---). Imidazole was added to the sample of inactive MnP at pH 4.5 to a final concentration of 5 mM (-•-). The inset shows the pH dependence of the absorption spectrum of inactive MnP. The ratio of absorbance at 412 nm to absorbance at 359 nm was plotted vs pH. The line drawn was a fit to the Henderson−Hasselbalch equation using a pK_a of 5.7.

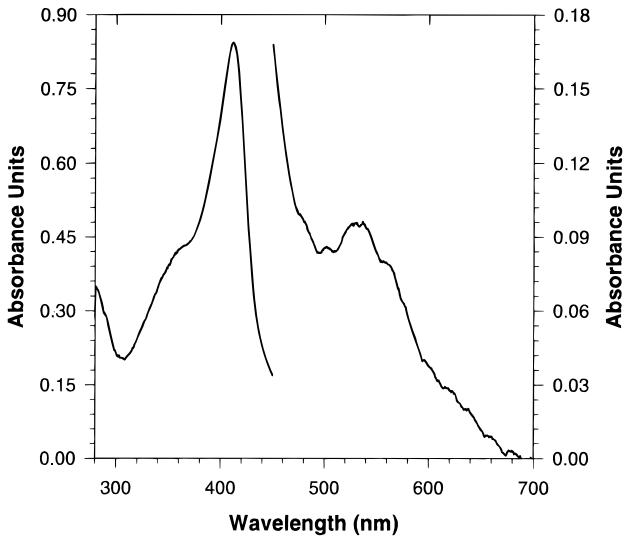

FIGURE 5: Absorption spectrum of D47A in the near-UV and visible regions. The sample contained approximately 10 μM Asp47Ala in 5 mM Tris, pH 8.0.

ellipticity with a maximum at 407 nm due to the heme Soret absorbance. Shown in panels B and C of Figure 9 are the CD spectra of MnP−CN and thermally inactivated MnP, respectively. The CD signal due to the Soret absorbance of MnP−CN exhibited large negative ellipticity with a maximum at 422 nm. However, inactive MnP had very weak and positive ellipticity in the Soret region.

DISCUSSION

Thermal Inactivation. In this investigation we have spectroscopically characterized the structural changes that occur in MnP during thermal incubation in the presence of

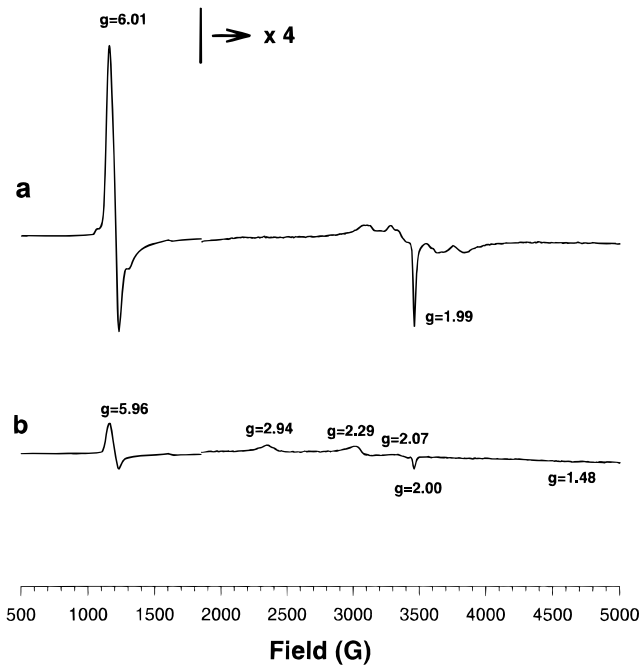

FIGURE 6: Low-temperature EPR spectra of active and thermally inactivated MnP. The samples contained (a) 250 μM active MnP and (b) 250 μM thermally inactivated MnP, prepared as described in the legend to Figure 1B and concentrated in 20 mM Tris, pH 8.0. Acquisition conditions were as follows: temperature, 10 K; microwave frequency, 9.65 GHz; microwave power, 1.01 mW; modulation amplitude, 5 G; modulation frequency; 100 kHz; time constant, 81.92 ms; conversion time, 81.92 ms; receiver gain, 1×10^4.

EGTA, which results in the release of calcium from, and inactivation of, MnP (Sutherland & Aust, 1996). There were clearly changes that occurred in the heme environment during this process. The red shift and decreased intensity of the Soret absorbance and the appearance of absorption maxima at 359, 533, and 562 nm were indicative of a conversion of the heme ferric iron from a high-spin pentacoordinate to a low-spin hexacoordinate complex (Hollenberg et al., 1980; Yonetani et al., 1966). There were isosbestic points observed in the absorption spectrum of MnP during thermal inactivation, indicating that the conversion of the active enzyme structure to the inactive enzyme structure occurred with no observed intermediates. Previously we had concluded that the decrease in absorbance of the Soret band was due to the loss of heme from the enzyme (Sutherland & Aust, 1996). In those previous experiments in which the absorption spectrum of MnP was monitored, the concentration of MnP was too low to check the spectrum at wavelengths greater than 450 nm and the enzyme was only inactivated to 25% at pH 6.5. Therefore the only change observed in the absorption spectrum of MnP was a decrease in heme absorbance at 407 nm. The conclusion that this was due to the loss of heme was supported by the observation that enzyme was only reactivated to 60% activity with calcium. However, under the conditions utilized for the reactivation experiments in this study, using EGTA, higher enzyme concentration, and a lower temperature of incubation following the addition of calcium, it was possible to reactivate MnP to 91% of the original activity (from 2%). In addition, the absorption spectrum of inactive MnP reverted to that of active enzyme, with peaks at 407, 504, and 637 nm, upon reactivation with calcium. This indicated that during the inactivation and loss of calcium from MnP, the decrease in

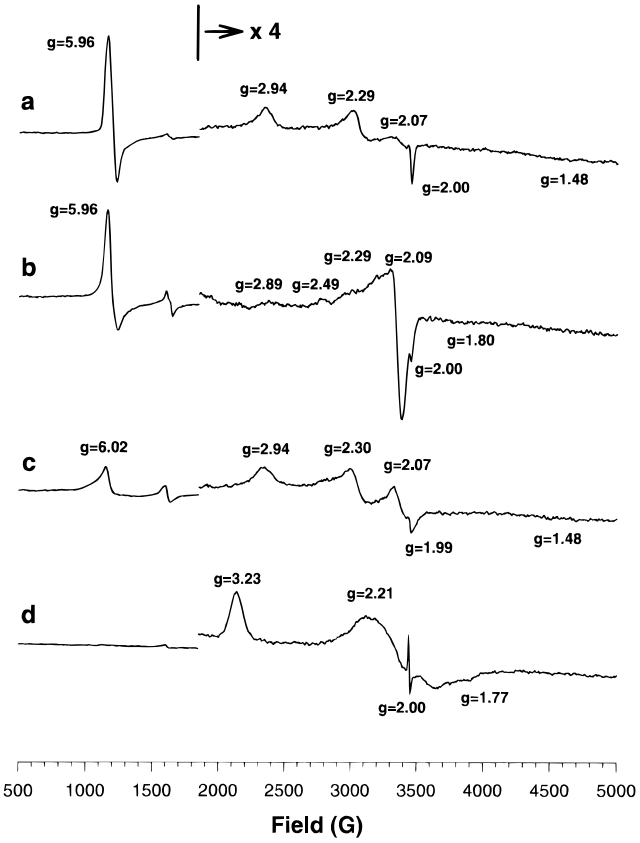

FIGURE 7: Low-temperature EPR spectra of thermally inactivated MnP, D47A and MnP−CN. (a) Inactive MnP prepared as described in the legend to Figure 7; (b) inactive MnP from (a) with pH adjusted to 4.5 with phosphate buffer; (c) D47A in 20 mM Tris, pH 8.0; (d) active MnP in 20 mM Tris, pH 8.0, and 10 mM potassium cyanide. All enzyme concentrations were 250 μM. Acquisition conditions were as described in the legend to Figure 7.

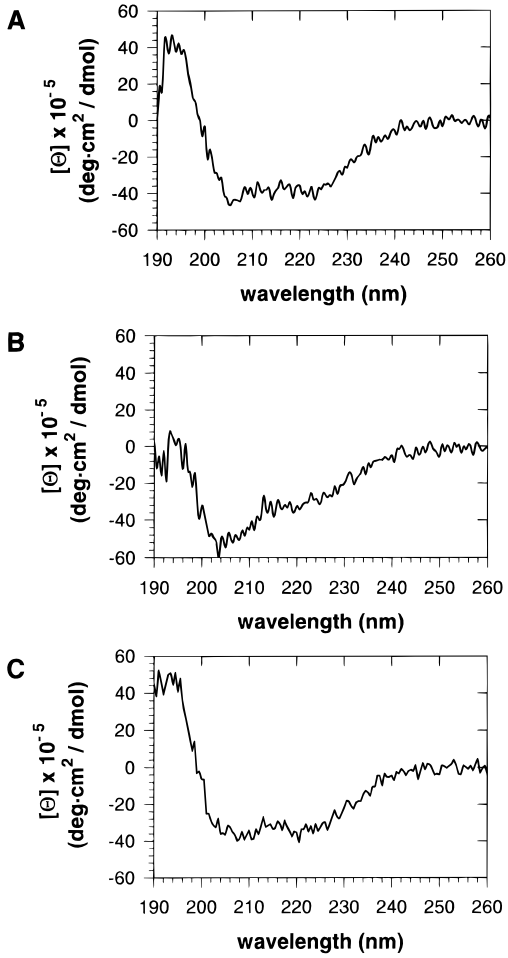

FIGURE 8: Circular dichroism spectra of MnP in the far-UV region. (A) Active MnP; (B) thermally inactivated MnP prepared as Figure 1B; (C) MnP reactivated with calcium as described in the legend to Figure 1B.

heme absorbance was not due to loss of heme. Rather, the heme environment of MnP was significantly altered such that the extinction coefficient decreased. However, the effects of thermal incubation on both the structure of the heme environment and the activity were reversed with calcium.

Compound I Formation. To further investigate the effects of the change in heme environment caused by thermal inactivation, the reaction of ferric enzyme with H_2O_2 was studied and it was shown that thermally inactivated MnP did not form compound I. In active MnP, this reaction is believed to occur in the distal heme pocket and to involve His46 and Arg42 (Dunford, 1991; Sundaramoorthy et al., 1994). Therefore, the distal heme environment, and in particular the interaction between the heme iron and these amino acid residues, was disrupted in the thermally inactivated MnP. This was consistent with the hypothesis that the distal calcium was lost during thermal inactivation and that the role of this calcium was to maintain the structural integrity of the distal heme environment, in particular helix B, which contains His46 and Arg42.

Cyanide Derivatives of MnP. Since the absorption spectrum of thermally inactivated MnP appeared to be similar to that of other low-spin ferric heme proteins, cyanide was utilized to prepare a low-spin derivative of MnP. The absorption spectrum of the MnP−CN had features similar to thermally inactivated MnP and other low-spin ferric heme proteins (Hollenberg et al., 1980; Yonetani et al., 1966). It was proposed that if the change in the heme environment of thermally inactivated MnP was due to the binding of a sixth iron ligand, then in the presence of excess cyanide, the sixth ligand may be replaced by cyanide and the absorption spectrum would be the same as that of MnP−CN. Indeed, the absorption spectrum of thermally inactivated MnP was altered significantly upon the addition of cyanide and was similar to that of MnP−CN. This demonstrated that heme was not lost during thermal inactivation and further supported the proposal that thermal inactivation of MnP caused predominantly a change in the heme environment due to acquiring a sixth ligand to the iron. However, the spectra of the cyanide adducts of active and inactive MnP were not identical, indicating there were still other slight differences in the heme environment. These slight differences may be due to an interaction between the iron-bound cyanide and a distal amino acid residue which may have previously been the sixth iron ligand in thermally inactivated MnP. The absorption spectrum of the cyanide adduct of inactive MnP in the presence of excess imidazole was very similar to that of inactive MnP. This suggested that the sixth iron ligand of inactive MnP was histidine.

pH Dependence of the Absorption Spectrum of Inactivated MnP. Thermally inactivated MnP exhibited a pH-dependent transition that was monitored by optical absorption spectroscopy. This transition, which did not occur in active MnP, had a pK_a of 5.7. The structure of the heme environment of

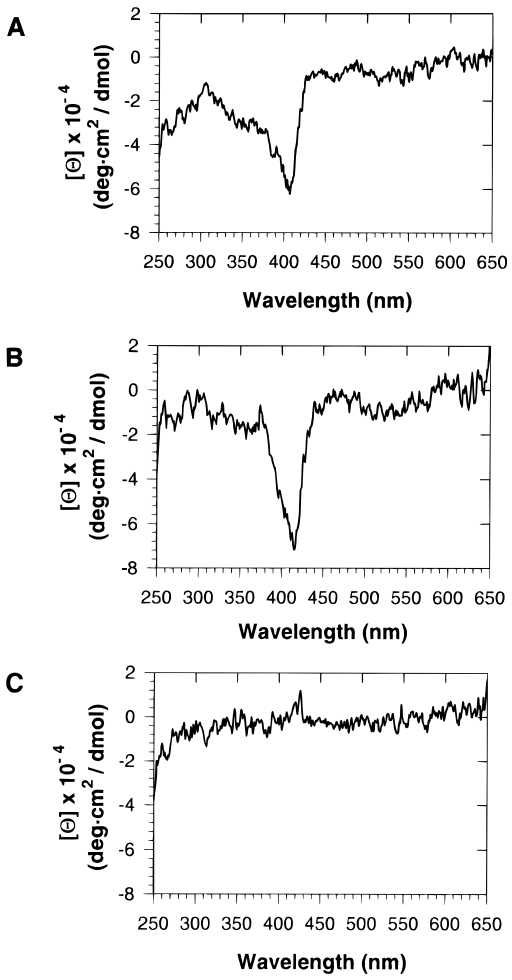

FIGURE 9: Circular dichroism spectra of MnP in the near-UV/visible regions. (A) Active MnP; (B) MnP−CN prepared as in Figure 3A; (C) thermally inactivated MnP prepared as described in the legend to Figure 1B.

cytochrome *c* peroxidase (CCP) and all CCP mutants except H52L, have also been shown to be dependent on pH (Smulevich et al., 1991; Turano et al., 1995; Vitello et al., 1993; Yonetani et al., 1966). The pH-dependent transition in CCP involved the ligation of the distal histidine (His52) to the heme iron (Smulevich et al., 1991). In all cases the resulting low-spin bis(imidazole) complexes had absorption spectra similar to inactive MnP with absorption maxima at ~533 and 563 nm (Smulevich et al., 1991). We propose that the ligation of His52 to the iron was possible in active CCP because it did not contain calcium to maintain the heme environment structure (Poulos et al., 1980). Only thermally inactivated MnP, in which calcium was removed, existed as a low-spin species in this pH range. The loss of the distal calcium may have allowed for movement of the α-helix containing His46 and liganding of His46 to the iron. It was proposed that the pH-dependent transition observed in inactive MnP was due to the protonation of His46, which disrupted the direct liganding of His46 to the heme iron and resulted in the formation of a complex with water bridged between the heme iron and His46. The proposal that a histidine was the sixth iron ligand in inactive MnP, at pH 7.5, was further supported by the observation that the addition of excess imidazole to inactive MnP at pH 4.5 resulted in a complex with an absorption spectrum almost identical to that of inactive MnP at pH 7.5. No such change was observed in the absorption spectrum of active MnP following the addition of imidazole. It was probably only possible for imidazole to access the distal heme environment of MnP following the removal of the distal calcium, which may allow the protein to be more flexible.

Spin State of MnP. The low-temperature EPR spectra for active MnP and MnP−CN demonstrated that these species were completely high-spin and low-spin, respectively. As predicted from the absorption spectra, thermally inactivated MnP, at pH 7.5 and 4.5, had slightly different heme environments but both were predominantly low-spin.

Circular Dichroism. The amount of α-helical structure (35%) present in active MnP was accurately predicted by computational analysis of the far-UV CD spectrum. The CD spectra of inactive and calcium-reactivated MnP indicated that there were clearly some changes in the protein structure that occurred upon inactivation and that the changes were reversible. Following the reactivation of the enzyme with excess calcium, the protein structure, as monitored by CD, was the same as that of the original active enzyme. The difference in the far-UV CD spectrum of inactivated MnP may be due to a loss of α-helical structure, from 35% to 26%, as predicted by computational analysis; however, the computer-generated fit to the spectrum was poor for inactive MnP. We attribute the difference in the spectra to a disruption of the α-helices that were structurally maintained by calcium lost during inactivation. Of particular importance to the activity of MnP is the structure of helix B containing His46, which could be disrupted due to the loss of the distal calcium.

If His46 was directly bound to the heme iron in thermally inactivated MnP, at pH 7.5, the protein would have a very symmetric bis(imidazole) heme structure. The hydrogen bonding of the δN1 of the two histidine ligands would further extend the symmetry. Analysis of the crystal structure of MnP showed that the proximal ligand, His173, was hydrogen-bonded to Asp242 and that the distal His46 was hydrogen-bonded to Asn80 (Sundaramoorthy et al., 1994). The predicted symmetry was demonstrated in the CD spectrum of inactive MnP in the near-UV/visible region. While the extinction coefficient of the Soret absorbance maximum of inactive MnP was 68% that of active MnP, the ellipticity, which is more sensitive to changes in symmetry, was barely detected for inactive MnP. Such an effect on the symmetry and CD spectrum of the heme was not purely due to the binding of a sixth ligand and conversion to a low-spin state. The CD spectrum of the low-spin cyanide adduct of MnP exhibited an ellipticity comparable to the original high-spin pentacoordinate heme protein.

Characterization of D47A. The role of the distal calcium in maintaining the distal heme environment was further investigated by determining the effect of changing the aspartate in this calcium binding site to alanine. It was predicted that the resulting protein, D47A, would have a lower affinity for calcium in the distal binding site and thus may be similar in structure to thermally inactivated MnP which contained only one calcium, believed to be in the proximal calcium binding site. Indeed, D47A had the same characteristics as thermally inactivated MnP. The protein was inactive under steady-state conditions and did not form compound I in the presence of H_2O_2. In addition, the absorption spectrum of D47A, with maxima at 359, 412, 533, and 561 nm, was the same as that for thermally inactivated MnP and the low-temperature EPR spectrum confirmed that

the protein was predominantly low-spin with a similar heme environment as inactive MnP. While the structural changes in thermally inactivated MnP could be reversed by calcium, calcium had no effect on D47A. To confirm that the distal calcium binding site of MnP was disrupted by the conversion of aspartate to alanine, the calcium content of D47A was analyzed, and indeed, it only contained one calcium.

The properties of D47A demonstrated that the same structural changes could be incurred either through alteration of the distal calcium binding site or through thermal inactivation resulting in the loss of calcium. This provides very strong evidence to support the proposal that the structural changes which occurred in MnP during thermal inactivation were due to the loss of the distal calcium, which must be important for maintaining the integrity of the heme environment. This was also consistent with the spectroscopic data and indicate the formation of a low-spin, symmetric, bis(imidazole) heme complex. The formation of such a complex was best explained by the movement of helix B, no longer structurally maintained by the distal calcium, such that His46 would be capable of liganding the heme iron, rendering MnP inactive.

Summary. It has been reported that many peroxidases contain calcium and it has been predicted that calcium maintains the structural stability of these enzymes (Booth et al., 1989; Haschke & Friedhoff, 1978; Hu et al., 1987; Poulos et al., 1993; Shiro et al., 1986; Sundaramoorthy et al., 1994; van Huystee et al., 1992). However, it appears that the role of calcium in other peroxidases may be different than in manganese peroxidase. Both horseradish and cationic peanut peroxidase contain two calciums, but the calcium was completely removed from horseradish peroxidase and cationic peanut peroxidase and the enzymes were still 40% and 50% active, respectively (Haschke & Friedhoff, 1978; Shiro et al., 1986; Hu et al., 1987; van Huystee et al., 1992; Schuller et al., 1996). Horseradish peroxidase without calcium was shown to have some low-spin character but the rate of compound I formation was not affected (Shiro et al., 1986). The complete removal of calcium from cationic peanut peroxidase had very little effect on the absorption spectrum (Maranon et al., 1993). Although the calcium binding sites of horseradish peroxidase have not been identified, the recently solved crystal structure of peanut peroxidase has been proposed to be a model for horseradish peroxidase (Schuller et al., 1996). The two calcium binding sites identified in peanut peroxidase were in the same position as the distal and proximal calcium binding sites of MnP and LiP. However, when compared to MnP, the distal calcium binding site of peanut peroxidase had some unique properties. First, the distal calcium was liganded by amino acid residues and one water molecule, compared to two water ligands in MnP. This may explain why more rigorous conditions were required to remove calcium from peanut peroxidase. Second, adjacent to the calcium ligands, Asp43 and Asp50, there was a disulfide bridge between Cys44 and Cys49 that formed a short loop. In MnP, this loop was shown to be much longer and did not contain a disulfide bridge. The presence of this disulfide bridge may explain why the heme environment and activity of peanut peroxidase was not affected as drastically as MnP following the loss of calcium.

We have shown previously that thermal inactivation of MnP resulted in the loss of calcium from the enzyme and that the process was prevented and reversed by calcium

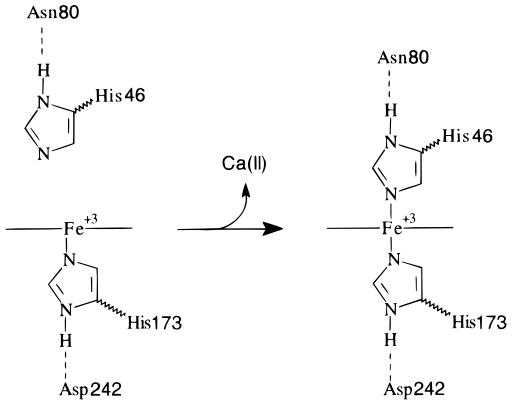

FIGURE 10: Diagram representing the proposed structural changes that occur in the heme environment of MnP during thermal inactivation.

(Sutherland & Aust, 1996). We have now provided evidence to explain why the release of calcium from MnP resulted in enzyme inactivation. Upon the thermal inactivation and loss of calcium from MnP, there was a distinct change in the heme environment and secondary structure of the enzyme that could be reversed by calcium. This structural change disrupted the distal heme environment of MnP and resulted in a sixth ligand to the distal side of the heme iron, converting the spin state of the iron from high-spin to low-spin. Further evidence was provided to suggest that the sixth ligand was His46. This amino acid residue exists above the heme iron in helix B, which is believed to be structurally maintained in active MnP by the calcium bound on the distal side of the heme (Sundaramoorthy et al., 1994). It was proposed that during thermal incubation the distal calcium was removed, which provided helix B more flexibility such that His46 liganded to the heme iron, rendering MnP inactive (Figure 10). This proposal was supported by the observation that D47A had the same calcium content and spectroscopic and catalytic properties as thermally inactivated MnP, except that D47A could not be reactivated with calcium. Therefore, disruption of the distal calcium binding site was sufficient to cause the same structural and activity changes to MnP as thermal inactivation. It was thus concluded that thermal inactivation was due to the removal of the distal calcium and that this calcium was required for activity because it maintained the structural integrity of the distal heme environment of MnP.

ACKNOWLEDGMENT

We thank Terri Maughan for secretarial assistance, Yixin Ben for production of MnP from *P. chrysosporium*, and Todd Butler for excellent technical assistance. We also thank Dr. Wes Sundquist and Allyson Christensen at the University of Utah for providing access to the circular dichroism spectrometer, Mary Hubbard of the Utah State University Analytical Laboratory for performing ICP analysis, and Dr. Rick Holz for his advice on EPR spectroscopy.

REFERENCES

Barr, D. P., & Aust, S. D. (1994) *Environ. Sci. Technol. 28*, 78A−87A.

Blumberg, W. E., Peisach, J., Wittenberg, B. A., & Wittenberg, J. B. (1968) *J. Biol. Chem. 243*, 1854−1862.

Booth, K. S., Kimura, S., Lee, H. C., Ikeda-Saito, M., & Caughey, W. S. (1989) *Biochem. Biophys. Res. Commun. 160*, 897−902.

Dunford, H. B. (1991) in *Peroxidases in Chemistry and Biology* (Everse, J., Everse, K. E., & Grisham, M. B., Eds.) pp 2−17, CRC Press, Boca Raton, FL.

Dunford, H. B., & Stillman, J. S. (1976) *Coord. Chem. Rev. 19*, 187−251.

Glenn, J. K., & Gold, M. H. (1985) *Arch. Biochem. Biophys. 242*, 329−341.

Glenn, J. K., Akileswaran, L., & Gold, M. H. (1986) *Arch. Biochem. Biophys. 251*, 688−696.

Haschke, R. H., & Friedhoff, J. M. (1978) *Biochem. Biophys. Res. Commun. 80*, 1039−1042.

Hollenberg, P. F., Hager, L. P., Blumberg, W. E., & Peisach, J. (1980) *J. Biol. Chem. 255*, 4801−4807.

Hu, C., Lee, D., Chibbar, R. N., & van Huystee, R. B. (1987) *Physiol. Plant. 70*, 99−102.

Kishi, K., Kusters-van Someren, M., Mayfield, M. B., Sun, J., Loehr, T. M., & Gold, M. H. (1996) *Biochemistry 35*, 8986−8994.

Kuan, I.-C., Johnson, K. A., & Tien, M. (1993) *J. Biol. Chem. 268*, 20064−20070.

Maranon, M. J. R., Stillman, M. J., & van Huystee, R. B. (1993) *Biochem. Biophys. Res. Commun. 194*, 326−332.

Millis, C. D., Cai, D., Stankovich, M. T., & Tien, M. (1989) *Biochemistry 28*, 8484−8489.

Poulos, T. L., Freer, S. T., Alden, R. A., Edwards, S. L., Skogland, U., Talaio, K., Eriksson, B., Xuong, N., Yonetani, T., & Kraut, J. (1980) *J. Biol. Chem. 255*, 575−580.

Poulos, T. P., Edwards, S. L., Wariishi, H., & Gold, M. H. (1993) *J. Biol. Chem. 268*, 4429−4440.

Schuller, D. J., Ban, N., van Huystee, R. B., McPherson, A., & Poulos, T. L. (1996) *Structure 4*, 311−321.

Shiro, Y., Kurono, M., & Morishima, I. (1986) *J. Biol. Chem. 261*, 9382−9390.

Smulevich, G., Miller, M. A., Kraut, J., & Spiro, T. G. (1991) *Biochemistry 30*, 9546−9558.

Sundaramoorthy, M., Kishi, K., Gold, M. H., & Poulos, T. L. (1994) *J. Biol. Chem. 269*, 32759−32767.

Sutherland, G. R. J., & Aust, S. D. (1996) *Arch. Biochem. Biophys. 332*, 128−134.

Tien, M. (1987) *CRC Crit. Rev. Microbiol. 15*, 141−168.

Tuisel, H., Sinclair, R., Bumpus, J. A., Ashbaugh, W., Brock, B. J., & Aust, S. D. (1990) *Arch. Biochem. Biophys. 279*, 158−166.

Turano, P., Ferrer, J. C., Cheesman, M. R., Thomson, A. J., Banci, L., Bertini, L., & Mauk, A. G. (1995) *Biochemistry 34*, 13895−13905.

van Huystee, R. B., Xu, Y., & O'Donnell, J. P. (1992) *Plant Physiol. Biochem. 30*, 293−297.

Vitello, L. B., Erman, J. E., Miller, M. A., Wang, J., & Kraut, J. (1993) *Biochemistry 32*, 9807−9818.

Wariishi, H., Akileswaran, L., & Gold, M. H. (1985) *Biochemistry 27*, 5365−5370.

Whitwam, R., & Tien, M. (1996) *Arch. Biochem. Biophys. 333*, 439−446.

Whitwam, R. E., Gazarian, I. G., & Tien, M. (1995) *Biochem. Biophys. Res. Commun. 216*, 1013−1017.

Yonetani, T., Wilson, D. F., & Seamonds, B. (1966) *J. Biol. Chem. 241*, 5347−5352.

BI962195M